THE ASTROPHYSICAL JOURNAL, 188:501–516, 1974 March 15

THE EVOLUTION OF SUPERNOVA REMNANTS. I. SPHERICALLY SYMMETRIC MODELS

ROGER A. CHEVALIER*
Princeton University Observatory, Princeton, New Jersey
Received 1973 August 31; revised 1973 October 11

ABSTRACT

The evolution of supernova remnants is studied using a spherically symmetric hydrodynamic code with a magnetic field approximately included. Properties of the emitted radiation are investigated. Particular attention is paid to the late phases when a dense neutral shell forms which accretes matter from both the interstellar medium and the hot interior. The shell absorbs hard ultraviolet and soft X-ray photons. The interstellar magnetic field produces the dominant pressure in the shell and determines its density and thickness. Results for explosions of 3×10^{50} ergs in gas of densities 10^{-2}, 10^{0}, and 10^{2} cm^{-3} show that harder radiation emerges from explosions in higher density gas. Using a scaling law, the results can be extended to a range of densities and initial energies. If cooling by collisionally heated grains occurs in the high-density case, about 20 percent of the total energy is radiated in the infrared in the early stages. In later phases, infrared cooling by radiation heated grains and infrared line emission may be significant, particularly in the low-density case. At the end of a typical run, the integrated radiated energy is about equally divided between infrared and ionizing radiation.

Interaction of the supernova shock with a large cloud decreases the total kinetic energy, and increases the thermal energy due to the reflected shock. The possibility that the initial supernova energy is deposited as relativistic particles is investigated; it is found that the shock radius a few thousand years after the explosion is fairly independent of the initial conditions, while differences when the radius is of order 1 pc are considerable. Comparison is made with observations. The observed relation between the surface brightness and diameter of old supernova remnants can be understood on the basis of the present models and van der Laan's theory for the radio emission.

Subject headings: hydrodynamics — supernovae — supernova remnants

I. INTRODUCTION

Supernova explosions are likely to be of considerable importance to the dynamics (Spitzer 1968) and ionization (Silk 1973) of the interstellar medium, and to observed galactic background radiation. Earlier work (Cox 1972*b*; Ostriker and Gunn 1971; Straka, Goldreich, and Sargent 1971; Rosenberg and Scheuer 1973) has indicated that the evolution of a supernova remnant in a uniform medium can be divided into a number of phases: first, the properties of the original explosion are important; then the heated interstellar matter has most of the energy and can be described by a similarity solution (Taylor 1950; Sedov 1959); and finally, radiative cooling results in the formation of a dense shell which "snowplows" into the interstellar medium, being driven from behind by hot gas.

The first part of this paper will take the Sedov solution as the starting point and examine the subsequent evolution in a uniform medium. The new features of this work are (*a*) the evolution is followed to times considerably past shell formation with the hydrodynamic code; (*b*) ionization and recombination of hydrogen are included; (*c*) a magnetic field is approximately included; (*d*) a range of initial conditions is taken; (*e*) absorption of ionizing radiation by the dense shell is investigated; and (*f*) attention is paid to the spectrum of emitted radiation. Even if the initial explosion is asymmetric, once the interstellar mass accreted is larger than the ejecta mass the remnant should tend toward spherical symmetry on a hydrodynamic time scale if the external medium is uniform. Considering the early evolution of the remnant to be described by a piston given a certain momentum, Rosenberg and Scheuer (1973) have found the Sedov solution is obtained once $M_{\rm IS}/M_{\rm piston} \gtrsim 40$ for their standard case. In this paper (§ V) we will consider the early stages with a relativistic gas behind the piston as in the model of Ostriker and Gunn (1971), and compare the results with a model like that of Rosenberg and Scheuer.

Old supernova remnants show a great deal of structure, presumably due to the inhomogeneity of the interstellar medium (see Sgro 1972 for theoretical work) and instabilities in the flow. Although interaction of the explosion with a cloud cannot be correctly modeled with a spherically symmetric code, it is possible to investigate the effects of a jump in density in the ambient medium (§ IV). Any realistic interpretation of the observations would involve dropping spherical symmetry and a detailed study of instabilities and turbulence behind the shock; however, some general comments are made based on the present models in § VI. The conclusions are in § VII. Subsequent papers will deal with nonspherical models and more detailed comparison with observations.

* Present address: Kitt Peak National Observatory, Tucson, Arizona.

II. EQUATIONS AND METHOD

The basic equations used in this investigation were:

$$\frac{d\rho}{dt} = -\rho\nabla\cdot v\,, \tag{1}$$

$$\rho\frac{dv}{dt} = -\nabla\rho + F_M\,, \tag{2}$$

$$\rho\frac{dU}{dt} = -\rho\mathscr{L} + \frac{p}{\rho}\frac{d\rho}{dt} + \nabla\cdot(\kappa\nabla T)\,, \tag{3}$$

$$p = n_{\rm tot}kT\,, \tag{4}$$

$$\frac{dx}{dt} = -n_e x\alpha^{(2)}(T) + \zeta(1-x) + (1-x)n_e C(T)\,, \tag{5}$$

and an equation for the magnetic field (cf. eqs. [6]–[9]), where F_M is the magnetic force per cm^3, U is the internal energy per gram including thermal and ionization energy, $\mathscr{L}$ is the net power loss per gram, κ is the coefficient of thermal conductivity, $n_{\rm tot}$ is the total density including helium, n_e is the total electron density, x is the ionized fraction of hydrogen, $\alpha^{(2)}(T)$ is the hydrogen recombination coefficient excluding recombinations to the ground state, ζ is the photoionization rate including both direct photoionization and ionization by secondaries, and $C(T)$ is the hydrogen collisional ionization coefficient. The ratio of helium to hydrogen number density, $n_{\rm He}/n$, was assumed to be 0.1. The equilibrium calculations of the ionization of He by Cox and Tucker (1969) were used in estimating the number of electrons contributed by ionized helium.

The equations were written in finite-difference form, so that both the spatial structure and time evolution were computed. A Lagrangian code with spherical symmetry was adapted from one written by Dr. Robert Stein.

a) Treatment of the Magnetic Field

Since the hydrodynamic scheme imposed spherical symmetry, the magnetic field could be treated only approximately; two methods were investigated.

First, assuming the flow is very turbulent so that the field is everywhere isotropic, the field produces an additional pressure and

$$F_M = -\frac{2}{3}\frac{d}{dr}\left(\frac{B^2}{8\pi}\right)\,, \tag{6}$$

the field is related to the density by

$$B^2\rho^{-4/3} = \text{const.}\,, \tag{7}$$

which closes the set of equations.

In the present problem, the field is likely to be preferentially compressed tangential to the supernova remnant shock. If a uniform field is initially present, and averages are taken over a sphere, the radial component of the magnetic force is

$$F_M = -\frac{d}{dr}\left(\frac{B_T^2}{8\pi}\right) - \frac{B_T^2}{4\pi r}\,, \tag{8}$$

where B_T is the tangential field. Now in addition to the magnetic pressure, there is a tension term, which had a negligible dynamical effect in the calculations. The equation for the tangential field is

$$B_T 2\pi r\Delta r = \text{const.}\,, \tag{9}$$

where Δr is the thickness of a Lagrangian spherical zone. The equation expresses conservation of tangential flux, good as long as there is no shearing of the field on a scale greater than Δr, and ohmic dissipation is negligible, which is almost certainly true under interstellar conditions.

The condition $\nabla\cdot B = 0$ gives the equation for the radial field

$$B_r r^2 = \text{const.} \tag{10}$$

Since the present problem involves an expansion, B_r decreases with time and will not be of any consequence for regions in which Δr of a zone increases less than r, which is true for all regions of interest.

Equation (8) can also be obtained on the assumption that the field is tangled on a scale smaller than the characteristic scale of the supernova remnant (Shapiro 1973). The possibility that the galactic magnetic field is cellular has been discussed by Michel and Yahil (1973). The only difference between the uniform and tangled-field approaches is that the first has $B_{T_0} = B_0\pi/4$, while the second has $B_{T_0} = B_0(2/3)^{1/2}$ for the initial field. The second expression was used in this paper; by multiplying any quoted field by 1.04, the uniform field can be obtained.

The computations showed that the magnetic field never was energetically important unless the postshock magnetic pressure exceeded the thermal pressure so that the magnetic field impeded the shock compression. Except in one model, this did not occur during a run; thus, in general, the magnetic energy grew to at most a few percent of the total initial energy. However, the field was important in the dense shell, where magnetic pressure dominated in the late stages. Computations were performed using both types of approximation, and the only difference between the two was in the maximum density reached in the dense neutral shell and its thickness. The second type of field allows less compression since the tangential field component becomes greater than the radial; the amount of compression expected is discussed in § III*a*. An observation which supports the second type of field is that radio polarization studies indicate a magnetic field tangential to the shell in several old supernova remnants (Woltjer 1972). The remainder of this paper assumes a tangled (or uniform) magnetic field.

b) The Energy and Ionization Equations

The net power loss per gram can be broken up into three terms:

$$\mathscr{L} = \mathscr{L}' + \frac{nx^2\alpha^{(2)}}{1.4m_{\rm H}}(\langle E_r\rangle + 13.6\ \text{eV}) - \frac{(1-x)}{1.4m_{\rm H}}\sum_i \zeta_{d_i}(\langle E_h\rangle_i + 13.6\ \text{eV}), \quad (11)$$

where the first term is the radiative loss except for hydrogen recombination, the second term is the loss due to radiative recombination of hydrogen, and the third is heating by secondary electrons resulting from photoionization. As described in § III*d*, the emergent energy spectrum was calculated for a number of frequency bins each characterized by a certain energy, $\langle E_e\rangle_i$, for the emerging radiation. $\langle E_h\rangle_i$ is the mean energy which goes into heat for each hydrogen photoionization, considering photons from frequency bin i, and ζ_{d_i} is the direct photoionization rate. $\langle E_r\rangle$ is the mean energy of the recombining electron and can be approximated as kT, from which deviations are small (cf. Spitzer 1948). The use of $\alpha^{(2)}(T)$ for the recombination coefficient is valid provided the gas is optically thick to Lyman continuum radiation, a good approximation in the regions where recombination occurs. Values for $\alpha^{(2)}$ are given in Spitzer (1968).

The input for the photoionization rate did not include any sources outside the supernova remnant, but only radiation due to the cooling of the heated material. The effect of photoionization was investigated in an approximate way, assuming that the whole remnant was optically thin to the ionizing radiation and judging the changes that occurred. The ionization rate in a zone with radius r was taken to be

$$\zeta_{d_i} = \frac{L(\langle E_e\rangle_i)\sigma(\langle E_e\rangle_i)}{4\pi r^2\langle E_e\rangle_i}, \quad (12)$$

where $L(\langle E_e\rangle_i)$ is the luminosity calculated for the energy bin i and σ is the absorption cross-section. Ionization rates were computed for two energy ranges, 13–41 eV and 41–410 eV. Beyond 410 eV, the luminosity of all the models decreases and the absorption cross-section became small. The mean energy in the first range was about 26 eV, which was sufficiently low that ionization by secondaries could be neglected. The mean energy for the second range was taken to be 100 eV; data on the heat and the number of secondary ionizations produced per photoionization are given in Dalgarno and McCray (1972). The fact that helium recombination produces a photon capable of hydrogen ionization was taken into account.

Using the coefficient of thermal conductivity for an ionized plasma with no magnetic field (Spitzer 1962, eqs. [5-47] and [5-48]), rough analysis showed that the conductivity term is most important in the early stages when the temperatures are high, but is small later in the adiabatic phase. When the term was included in the numerical integrations, it led to numerical fluctuations ($\sim$10 percent) which were much larger than any change the conduction brought about. Cox (1972*b*) has drawn the conclusion that heat conduction affects the expansion dynamics very little. If the conduction is perpendicular to a magnetic field, it becomes entirely negligible (Spitzer 1962, eq. [5-53]). The neutral shell which formed due to thermal instability did have sharp changes in thermal gradient at its edges. Yet the neutrals are tied by collisions to the ionized particles which are constrained by the primarily tangential field in the dense shell. In the results which follow, heat conductivity has been neglected.

c) Radiative Cooling

In this section, we discuss the term $\mathscr{L}'$ which appeared in equation (11), and which over most of the range of temperature and density can be expressed as

$$\mathscr{L}' = \frac{n}{1.4m_{\rm H}}\Lambda(x, T). \quad (13)$$

Calculations of the cooling function $\Lambda(x, T)$ for an optically thin gas in steady state in the temperature range 10^4 °–10^8 ° K have been performed by Cox and Tucker (1969) and Cox and Daltabuit (1971). The time-dependent problem has been examined by Kafatos (1972) for the temperature range 10^4 °–10^8 ° K, and by Jura and Dalgarno (1972) below 10^4 ° K.

A possibly important coolant above temperatures of about 10^6 ° K is infrared radiation by grains which have been collisionally heated (Ostriker and Silk 1973). The density of grains, under the conditions studied here, is uncertain; it appears that the process is energetically important only for an explosion in a high-density region. It was thus included only for the integration with $n_0 = 100\ \text{cm}^{-3}$. The expression used for the cooling was

$$\Lambda(T) = 5 \times 10^{-33}T^{3/2}\ \text{ergs cm}^3\ \text{s}^{-1}, \quad (14)$$

which neglects grain destruction (see Burke and Silk 1974). For explosions in a low-density medium, the fractional energy emitted is small enough that the Sedov solution remains a good description.

Kafatos (1972) has shown that above 10^6 ° K the assumption of a steady state is valid, so the ionization equilibrium results were used in this regime. The time-dependent cooling curve of Kafatos was used for cooling by electron excitation of ions in the temperature range 2×10^4 ° to 10^6 ° K. It is important that the ionization times not be much longer than the cooling times behind the shock. The data in Kafatos (1972) show that the ionization times are shorter. The assumption that photoionization of the impurities is unimportant also appears to be justified based on data given by Kafatos. Another question is whether the hydrodynamic times are shorter than the cooling and recombination times, which would bring the gas further from steady state. After integrations were performed, the hydrodynamic term was found to be smaller than the cooling term in the energy equation.

At low temperatures, electron excitation of neutral hydrogen, excitation of ions by electrons, and excitation of ions by neutrals were included separately since

each has a characteristic dependence on ionized fraction. Cooling rates were taken from Jura and Dalgarno (1972) and are reviewed in Dalgarno and McCray (1972); besides Lα, fine-structure transitions of C^+, O, Si^+, and Fe^+ and metastable transitions of O and N were included. Abundances were as in Schwarz, McCray, and Stein (1972). Again the question of recombination times is important. Schwarz (1973) notes that the highly charged ions recombine quickly, and that absorption is most likely to occur by hydrogen and helium under the conditions he studied, which are similar to those in the present investigation.

The above cooling rates are based on the assumption that every upward collisional transition results in a radiative decay. Upper levels can also be depopulated by collisions, which will dominate at densities above that at which the collisional and radiative de-excitation rates are equal. The radiative rates were taken from Field *et al.* (1968) and Wiese, Smith, and Glennon (1966). The collisional rate can be calculated on the assumption that the two levels are populated as in thermodynamic equilibrium. The lowest critical densities are for C^+: $n_{\rm H\,I} = 3000\ {\rm cm}^{-3}$ and $n_e = 8.7\ {\rm cm}^{-3}$ for excitation by atomic and electron impact, respectively, assuming $T_e = 100°$ K. Since higher densities were encountered in the calculations, collisional de-excitation was accounted for in an approximate fashion. The emissivity in each line was assumed to go as n^2 up to the critical density, above which it went as n. The approximation made is that almost all the atoms and ions are in the ground level; the error in the cooling rate is $n_{\rm total}/n_{\rm lower}$ which can be as large as a factor 3 for C^+.

In addition to the uncertainties and inaccuracies already mentioned, the element abundances in interstellar space may vary by more than an order of magnitude, the cross-sections used in the cooling rates are uncertain, and there may be heating or cooling processes which have been entirely neglected; specific parts of the cooling curve will be affected. The appearance of a supernova remnant may depend on local conditions in the surrounding medium besides the gas density.

d) The Emergent Energy Spectrum

Every 10 time steps, the amount of energy radiated was computed for each zone and was used in conjunction with the temperature of each zone to roughly calculate the emergent energy spectrum on the assumption that the remnant was optically thin at all wavelengths. The frequency of the radiated energy for each zone was estimated and the energy was added to one of 21 frequency bins ranging from $\nu = 10^{11.5}$ to $10^{22.0}$ Hz in intervals of a factor of $10^{0.5}$ in frequency. In addition to the instantaneous luminosity, the integrated energy was calculated. After the formation of the neutral shell, the luminosities from inside and outside the shell were calculated separately. The frequency of the radiation as a function of temperature was estimated at high temperatures from the work of Tucker and Koren (1971), Cox and Tucker (1969), Cox and Daltabuit (1971), and Kafatos (1972). In the low-temperature regime, the computed cooling term specifically included all the transitions, so that the relative contribution of each transition could be calculated as a function of temperature.

In the above estimates, all the radiation from regions below $10^{6.7}$ ° K is assumed to appear as line emission, yet there is also a thermal continuum component at each temperature. This was calculated separately over the frequency range $10^{6.0}$–$10^{17.5}$ Hz, again in bins covering a factor $10^{0.5}$ in frequency. Considering the large range in temperature, the Gaunt factor was included in both the quantum-mechanical and classical limits depending on whether the temperature was more or less than 5.5×10^5 ° K (Oster 1961).

e) Initial Conditions and Computational Details

For the models of §§ III and IV, the energy was initially deposited as heat; the temperature dropped exponentially with radius. This relaxed to a good approximation of the Sedov solution within a few hundred time steps or about one doubling time. The models of §§ III and V assumed the temperature of the ambient medium to be 10^4 ° K and preionized.

The hydrodynamic code computed equations (1)–(3) explicitly and equations (4) and (5) implicitly. Artificial viscosity was used to damp fluctuations due to shock waves. The explosion was allowed to expand to a number of zones between 80 and 100 at which time rezoning was initiated. Without continual rezoning, the remnant would have expanded to several hundred zones after shell formation, making further progress impossible. During the Sedov phase, rezoning was performed interior to the newly shocked region, while during the snowplow phase all rezoning was within the dense shell. A check on the accuracy of the integration was provided by the total energy of the remnant, taking into account energy added from the ambient medium. The fractional error was always better than 1 percent at the end of a run and was often better than 0.1 percent.

III. RESULTS FOR A UNIFORM MEDIUM

Computer runs were performed for an explosion in a uniform medium with a range of densities likely to occur in interstellar space. Table 1 lists the initial parameters for each run, including the energy E_0, density n_0, and magnetic field B_0, as well as the maximum time reached, $t_{\rm max}$. Runs all had the same energy, 3×10^{50} ergs, but results for other energies can be obtained by scaling the computed results. The scaling law was found by expressing each of the physical quantities as λ to a power, substituting into equations (1)–(5), and solving for the powers; it has been previously noted by Sgro (1972). If the energy is multiplied by λ^{-2}, and the densities by λ^1, the same solution holds if lengths are multiplied by λ^{-1}, t by λ^{-1}, p by λ^1, T by λ^0, v by λ^0, B by $\lambda^{1/2}$, and luminosities by λ^{-1}. Since B is one of the initial conditions, it seems undesirable to have it change; yet B scales with ρ in a physically plausible manner and, as described in § III*a*, the effects of changes in the magnitude of B can easily be derived provided that the magnetic energy is a small fraction of the total. The scaling law holds as

TABLE 1

PARAMETERS OF MODELS*

PARAMETER	MODEL A	B	C	D	E	F
E_0 (ergs)	3×10^{50}	3×10^{50}	3×10^{50}	3×10^{50}	3×10^{50}	3×10^{50}
n_0 (cm^{-3})	1.	0.01	0.01	100.	100.	0.1, 5.
B_0 (gauss)	3×10^{-6}	3×10^{-6}	1×10^{-7}	1×10^{-5}	1×10^{-5}	3×10^{-6}
Grain cooling	no	no	no	no	yes	no
t_{max} (years)	5.1×10^5	1.8×10^6	2.0×10^6	1.4×10^4	6.0×10^3	3.6×10^5

* These can be scaled to a range of energies using the scaling law noted in § III.

long as the emissivity is proportional to $n^2\Lambda(T)$. From § II*c*, we know that this is not the case at high density and low temperature, but this will only affect the rate of cooling in the dense shell. Thus, results for a range of densities can be extended to a range of energies and densities; for example, models C and D can be scaled to models with $n_0 = 1$ cm^{-3}, and $E_0 = 3 \times 10^{46}$ ergs, $B_0 = 10^{-6}$ gauss; and $E_0 = 3 \times 10^{54}$ ergs, $B_0 = 10^{-6}$ gauss, respectively. Comments which apply to high densities for a series of models with the same energy, also apply to high energies for a series of models with constant ambient density.

To check the computing scheme, an adiabatic blast integration was performed for comparison with the results of Sedov (1959). Integration of analytical formulae given by Sedov shows that for a $\gamma = 5/3$ gas, 28.3 percent of the total energy is kinetic while 71.7 percent is thermal, somewhat different from the 20 percent, 80 percent cited by Spitzer (1968) and Cox (1972*b*). The shock radius follows the law $R = (2.02E_0/\rho_0)^{1/5}t^{2/5}$, where ρ_0 is the density of the interstellar medium. The computer results verified the energy fractions to a percent, and the radius relation was used to set the zero point in time of the integrations, since they were initiated at finite radius.

The qualitative evolution was essentially as described by Cox (1972*b*). The Sedov solution was set up, and the radiative cooling first had the effect of causing a temperature dip behind the shock front. As cooling became more important, the radius increased less rapidly than in the adiabatic solution and a dense neutral shell formed. The effect of cooling by collisionally heated grains is different since it decreases the temperature of the hot interior. First the run with $n_0 = 1$ cm^{-3} will be described in detail, then changes due to differences in external conditions will be taken up.

a) $n = 1$ cm^{-3}

The basic physical quantities p, n, v, and T for integration A as a function of radius are shown at five times in figure 1. At the first time, 2.05×10^4 years, radiative cooling was not yet important and the Sedov solution described the situation. Next, at 4.05×10^4 years, cooling had caused the temperature to drop in the outer part of the remnant, giving a decrease in pressure. Due to the ram pressure of the interstellar medium, a spike in pressure began to appear. Because of the drop in pressure behind the spike, hot material began to be accelerated toward the dense neutral shell which was forming. The shell formation was essentially complete by 4.55×10^4 years, when the density reached a maximum (fig. 2). Now the pressure spike was fully developed, and the pressure drop behind it accelerated material even more. The velocity maximum above the little notch, which indicates the speed of the dense shell, coincides with the pressure minimum. Later, shocks formed on both sides of the dense shell. Where the pressure minimum occurred, the temperature was low, a few times 10^4 ° K, and the material began to recombine; but when it hit the dense shell, it was reheated to about 10^5 ° K and was re-ionized. It soon recombined once more due to the higher densities. In the region where the pressure decreased with radius while the density increased, the flow is actually likely to be turbulent due to the Rayleigh-Taylor instability. An estimate of the amount of turbulent energy at 4.55×10^4 years is 4×10^{49} ergs, or ~ 1 percent E_0, assuming the region spans $r = 14.8$ to 17.0 pc with $n = 0.7$ cm^{-3} and $v = 140$ km s^{-1}. No attempt was made to account for this in the numerical scheme. Since a certain amount of the energy would go into transverse velocities, the force on the dense shell from inside would be reduced. This uncertainty should be kept in mind when quantitative estimates are made of how the remnant radius increases with time.

While the shell was forming, the gas recombined and cooled to about 10° K. Schwarz *et al.* (1972) found similar final temperatures in their study of the formation of interstellar clouds. Here the shell was entirely held up by magnetic pressure, the thermal pressure being negligible; in all regions outside that of high density, the thermal pressure dominated. In runs with no magnetic field, the thermal instability again ended with a temperature of about 10° K, but the densities were so high, about 10^4–10^5 cm^{-3}, that the zone size became very small and the Courant condition on the time step made further progress very slow. Except for the maximum density reached and the thickness of the dense shell, all the properties of the remnant evolution through shell formation were the same with or without the magnetic field.

With the tangled field of 3×10^{-6} gauss, the time step was limited by radiation and ionization-recombination time scales rather than the Courant condition, and the evolution could be followed beyond the time

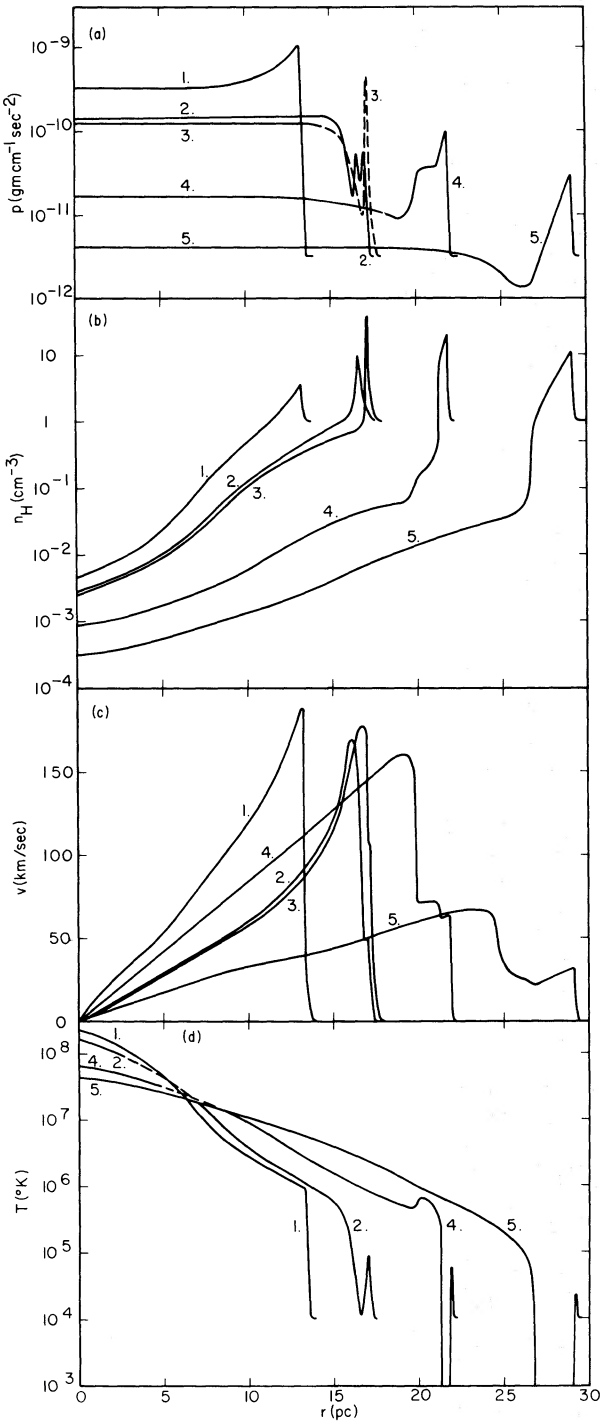

FIG. 1.—Profiles of (*a*) the sum of magnetic and thermal pressure, p; (*b*) hydrogen number density, n; (*c*) gas velocity, v; and (*d*) temperature, T, at five times in the evolution of a 3×10^{50} erg explosion in a medium with $n_0 = 1\ \mathrm{cm}^{-3}$ and $B_0 = 3 \times 10^{-6}$ gauss (model A). The times are (1) 2.05×10^4 years; (2) 4.05×10^4 years; (3) 4.55×10^4 years; (4) 1.00×10^5 years; and (5) 2.50×10^5 years. Time 3 is omitted on the T profiles for greater clarity. In the places where T drops below the plot, $T = 10°$ K.

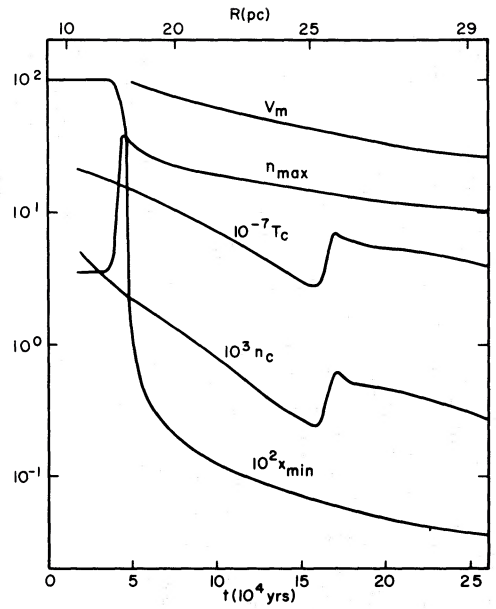

FIG. 2.—The peak density $n_{\max}$ (cm^{-3}), minimum ionized fraction $x_{\min}$, velocity of the dense shell v_m ($\mathrm{km\ s}^{-1}$), central density n_c (cm^{-3}), and central temperature T_c (° K) of model A as a function of time.

of shell formation. The drop in pressure behind the dense shell maintained itself as material at the outer edges cooled below the temperature that would characterize the Sedov solution. Thus the dip moved toward the remnant center with respect to Lagrangian mass zones. After 1×10^5 years (fig. 1), the shock velocity had decreased so the pressure in the dense shell fell, giving less compression. The dense shell was 0.6 pc thick with a radius of 21.6 pc. The pressure peak due to ram pressure was followed by a region of moderately high pressure, maintained by the acceleration of material into it. As the pressure dip moved toward the center of the remnant, the density in the region of the dip decreased so that the cooling of the region became less effective. Thus the velocities of the gas accelerated by the pressure dip decreased, and by 1.35×10^5 years they were no longer able to maintain the high pressure on the outside of the dip. A wave moved toward the center, increasing the pressure throughout the interior, and bounced at $r = 0$. The rise in central density and temperature can be seen in figure 2. After these dynamic effects damped out, the situation again became something like that at an earlier time, but now with the highest velocities right next to the dense shell region where cooling occurred to 10° K (last time in fig. 1).

In what follows, most of the attention is focused on the energetically important dense shell. Note that the central density had fallen to 3×10^{-4} of the interstellar value by 2.5×10^5 years, when the central temperature still exceeded 10^7 ° K. The cooling time for this material is considerably longer than the hydrodynamic time of the remnant.

Recombination proceeded in the dense shell quite

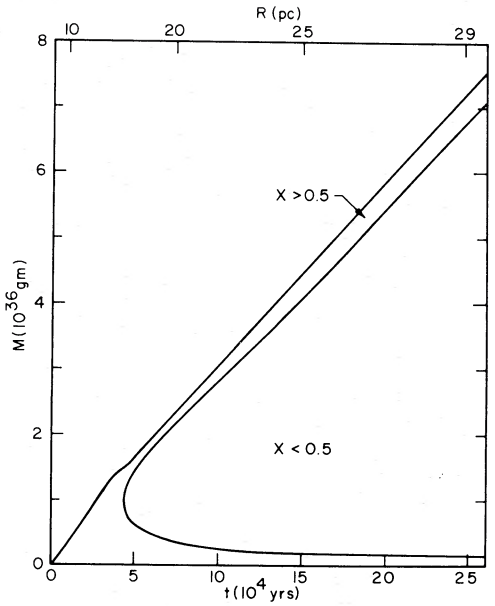

FIG. 3.—The distribution of neutral (ionized fraction x less than 0.5) and ionized mass in model A as a function of time and radius. The upper ionized mass is exterior to the dense shell, and the lower is interior.

rapidly (fig. 2). At later times, the majority of the mass was neutral (fig. 3). The interior ionized mass was always dropping since the gas ran into the dense shell and cooled, while the outer ionized mass increased slowly. The amount of outer ionized mass is proportional to R^2 times the thickness of the cooling region, which depends on the gas velocity relative to the dense shell times the cooling time for postshock material. The computations showed that the shock moves more rapidly than the dense shell. When most of the mass is in the neutral shell, we have

$$\eta \equiv r/\delta r \gtrsim 3\rho_s/\rho_0 , \qquad (15)$$

where δr and ρ_s are the shell thickness and density, respectively.

The time for gas to move from the shock to the recombination region was small compared with the time for the shock velocity to change significantly. Thus, as in Cox (1972*a*), the quantity $B_T^2/8\pi + \rho v^2 + n_{\rm tot}kT$, where v is the velocity in the shock frame, is expected to be constant through this region. This was found to be approximately true in the integration; in the later evolution, the magnetic pressure made up about 0.95 of the total and ρv^2 the rest in the dense shell. The velocity v for the shell depends on the rate of change of the thickness of the cooling region. Thus

$$B_s = (\epsilon 8\pi\rho_0)^{1/2} v_{\rm sh} , \qquad (16)$$

where ϵ is a constant somewhat less than 1 (0.95 in the case mentioned), B_s is the tangential field in the dense shell, and $v_{\rm sh}$ is the shock velocity. As long as large changes in radius do not occur, B_T is proportional to ρ, so with equation (15), η can be related to B_{T_0}, ρ_0, and $v_{\rm sh}$, yielding

$$\eta \approx 5.1 v_{\rm sh}/(v_{\rm A})_0 , \qquad (17)$$

where $(v_{\rm A})_0$ is the Alfvén velocity in the interstellar medium. For the turbulent field case,

$$\eta \approx 6.6[v_{\rm sh}/(v_{\rm A})_0]^{3/2} . \qquad (18)$$

The compression is greater than in the tangled field approximation. These expressions hold provided the magnetic pressure dominates in the dense shell; if not, then

$$\eta \approx 4.8(v_{\rm sh}/c_s)^2 , \qquad (19)$$

where c_s is the isothermal sound speed in the dense shell and is not well determined in the present computations since some heating sources may have been neglected.

The energetics of the explosion are described in figures 4–6 under the assumption that the remnant is optically thin to all radiation. The kinetic energy dropped slowly prior to shell formation, rose when material was accelerated into the dense shell, then continued to decrease (fig. 4). The amount of ionizing radiation emitted before shell formation is significant,

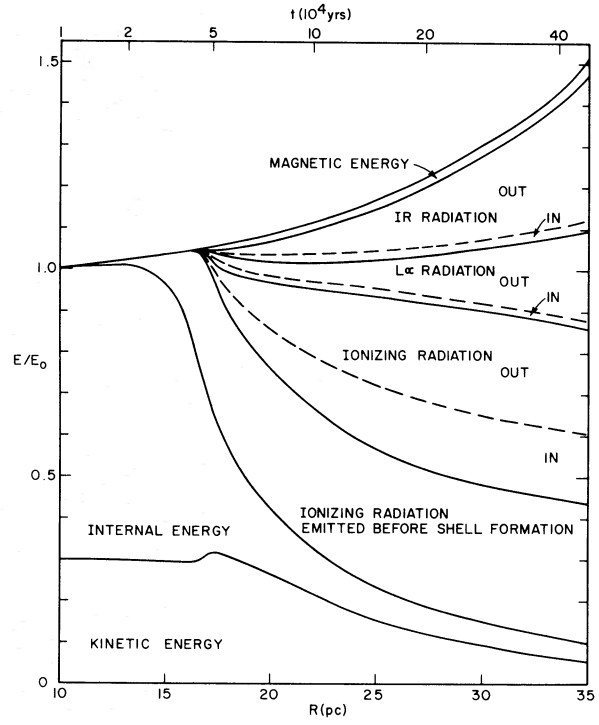

FIG. 4.—The energetics of model A as a function of remnant radius under the assumption that the remnant is optically thin at all wavelengths. Before $R = 10$ pc, the adiabatic solution holds. "In" applies to radiation emitted inside the dense shell, while "Out" applies to that emitted between the shock front and the dense shell. E/E_0 increases due to internal energy added by surrounding gas, assumed to be ionized and at $T = 10^4$ ° K.

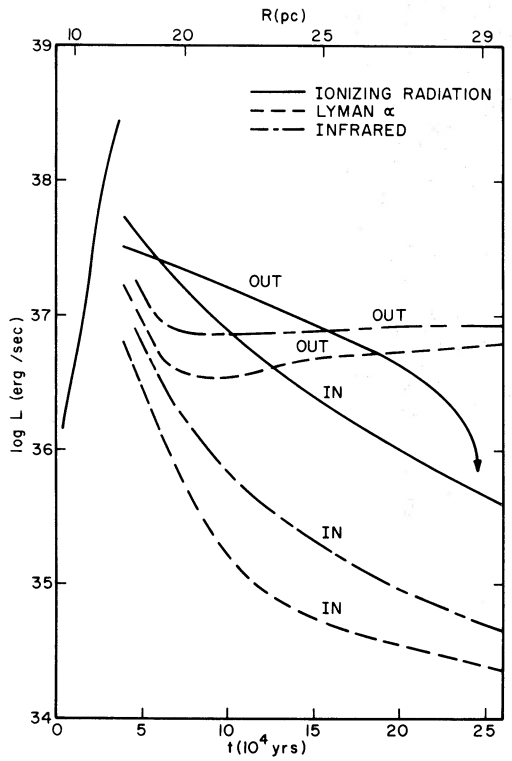

FIG. 5.—The luminosities of ionizing radiation, Lα, and infrared radiation in model A as a function of time under the assumption of small optical depth. The labels "Out" and "In" are as in fig. 4. The arrow on the "Out" ionizing radiation indicates that it goes to zero due to the decreasing postshock temperature.

$0.33E_0$. Lyman-α and the infrared lines only occurred once cooling in the dense shell began. The magnetic energy was always small, as noted before.

The emission of ionizing radiation by the hot interior brings up the question of the optical depth in the dense shell. Cross-sections for hydrogen and helium, the dominant absorbers, were calculated from Bethe and Salpeter (1957) and Brown (1971). The energy at which the shell thickness equals the photon mean free path was found to be about 50 eV when the remnant radius was 20 pc. If most of the mass is contained in the dense shell, its cross-section goes as R^{-1}; even if the remnant radius doubles, the critical energy will only increase to 60 eV.

The interaction of the ionizing radiation with matter in the dense shell was estimated by including photoionization as described in § II*b*. The effect during shell formation was to raise the ionized fraction by about 10 percent and to lower the temperature. Since the cooling is more efficient at high ionized fraction, the temperature dropped even with heat being added. Photoionization did not significantly change the timescale for shell formation, and the shell soon became optically thick to the hard-ultraviolet radiation (i.e., the approximation used in code broke down). After shell formation, the ionized fraction at the boundary of the shell was increased. Most of the energy of the absorbed ionizing radiation went into Lα radiation. Assuming a closed shell, most of the hard-ultraviolet radiation from inside the shell and approximately half that from outside would be absorbed, and reemitted at longer wavelengths.

The total energy which has emerged in the various frequency bins (fig. 6) permits a check on the assump-

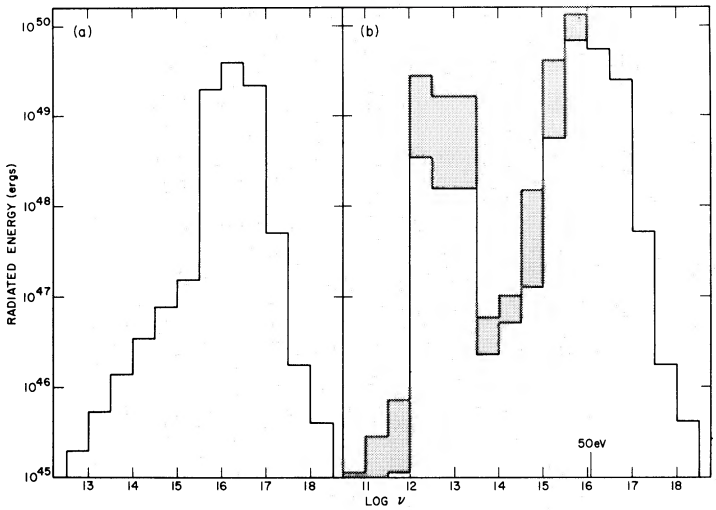

FIG. 6.—The distribution of radiated energy into frequency bins at two times for model A: (*a*) 3.55×10^4 years, shortly before shell formation when $0.269E_0$ has been radiated; and (*b*) 2.5×10^5 years, when almost all the ionizing radiation has been emitted and $1.094E_0$ has been radiated. The shaded parts refer to energy emitted after shell formation outside the shell. The energy marked in eV is approximately that at which the dense shell becomes optically thick.

tion that the medium outside the shock is preionized. Figure 6*a*, which has the energy emitted before shell formation, indicates that enough ionizing radiation was produced to ionize a region over 20 pc in radius. The structure of the ionized region is quite complicated since the more energetic photons will partially ionize a larger region: calculations of this process have so far only dealt with monoenergetic X-ray bursts (Schwarz 1973). After shell formation, ionizing radiation continued to be emitted; although by 2.5×10^5 years ($R = 29.24$ pc) most of the radiation was being emitted as Lα or in the infrared. The bin with the most energy was $\log \nu = 15.5$–16.0 (fig. 6*b*) or 13.1–41.3 eV, frequencies which are absorbed by the shell, so the radiation may be degraded to Lα or infrared photons. The rise in E/E_0 in figure 4 is due to the internal energy added by the interstellar medium. In the computer model, preionization did not result from the cooling radiation of the remnant, but was an assumption. By $R = 35$ pc, E had increased by over 50 percent (fig. 4). Is the ionizing radiation capable of heating and ionizing the external medium to this extent? If the dense shell is closed, it will absorb about half of the ionizing radiation emitted after shell formation, and the radiation which does get out will probably be insufficient. Then the incoming material is partially neutral and the situation described for run C in § III*b* applies. But if the cool material is clumpy and is not spread evenly over the shell, the absorption effects will be greatly reduced and the radiation may be capable of preionizing the medium.

The shell is optically thick to Lα radiation. At least three possibilities exist for the escape of this energy: (*a*) absorption of Lα by grains which subsequently emit in the infrared; (*b*) emission by the two-photon process; and (*c*) relative motions causing shifts in the wavelength of the radiation so it eventually escapes at wavelengths on either side of 1216 Å. Possibility (*a*) depends on the existence of grains. A simple estimate of whether grains will be disrupted by collisions with other grains in the shock based on the discussion in Spitzer (1968) shows that they should survive; collisions with thermal particles are unimportant. Auer (1966), who studied the transmission of Lα in a region with temperature in the range 10^2 ° to 10^4 ° K, found that the two-photon emission is negligible compared to (*c*); but if grains are present in their average abundance, then possibility (*a*) will be the dominant process. Figure 5 indicates that in the later part of the evolution, recombination Lα radiation from outside the dense shell is very important. It is possible that a significant fraction of this radiation will be converted to infrared frequencies by grains.

At late times, it is useful to express the remnant radius in the form $R \sim t^q$. There is some indication that q slowly decreases with time, going from 0.320 to 0.300 as thermal energy of the hot interior is lost to radiation. Estimates which become valid after about 5×10^4 years are

$$R = 21.9 t_5^{0.31 \pm 0.01} \text{ pc and } v_{sh} = 66.5 t_5^{-0.69} \text{ km s}^{-1}, \quad (20)$$

where t_5 is the age in 10^5 years. The kinetic energy of the remnant can be estimated at the time the shell velocity has slowed to 14 km s^{-1}, the rms velocity of interstellar clouds (Spitzer 1968), and is found to be 4 percent of the total initial energy, close to Spitzer's (1968) rough estimate of 3 percent.

The high densities in the dense shell suggest the possibility of star formation. A rough criterion can be derived for the radius, a, of a section of a thin homogeneous sheet at which the self-gravitational energy will dominate the thermal or magnetic energy:

$$a > 0.5 \frac{p}{G \rho_s^2 \delta r}, \quad (21)$$

where p is the thermal pressure in the sheet (here, the dense shell) and G is the gravitational constant. If p is the magnetic pressure, the coefficient becomes 0.3 rather than 0.5. It is necessary that a be less than the radius of the remnant. Using relations from the above discussion, this can be reduced to a condition on the number density in the dense shell

$$n_s > 3 \times 10^4 t_5^{-2} \text{ cm}^{-3}. \quad (22)$$

The result is independent of initial conditions. We see that the gravitational energy will be important only in the absence of magnetic field effects. The requirement that the growth time of the gravitational instability (i.e., the free-fall time) be less than the remnant age again indicates the necessity of very high densities. If weak field regions exist and star formation can occur, the expected observational result would be an expanding ring of stars.

After shell formation, the outer regions gave most of the radio bremsstrahlung flux (fig. 7). In terms of

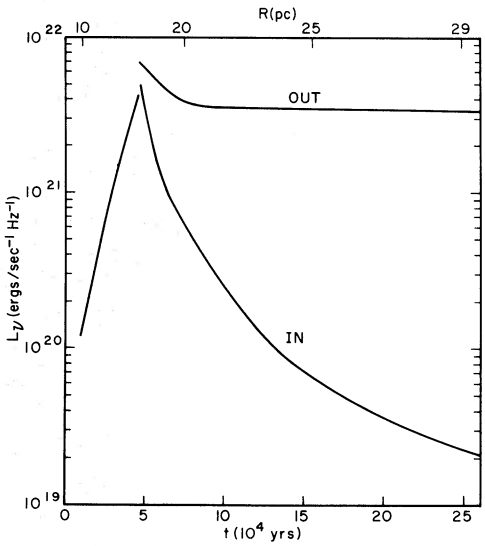

FIG. 7.—The luminosity per Hz of bremsstrahlung radiation at 1 GHz for model A.

the plotted quantity, the observed flux is

$$0.84L_{21}/R_{\rm kpc}{}^2 \text{ f.u.}, \quad (23)$$

where L_{21} is the luminosity per hertz at 1 GHz in 10^{21} ergs s^{-1} Hz^{-1}, $R_{\rm kpc}$ is the distance to the remnant in kiloparsecs, and a flux unit is 10^{-26} W m^{-2} Hz^{-1}. The predicted thermal flux is on the order of a percent of total observed remnant fluxes (cf. Woltjer 1972). After shell formation, the flux from the outer cooling region remained fairly constant, while that from the inner region decreased steadily due to the decreasing interior density. At low frequencies, the bremsstrahlung spectrum was relatively flat but had some slope due to the temperature and frequency dependence of the Gaunt factor; if flux is proportional to ν^{α}, $\alpha \approx -0.1$. The frequency at which the spectrum became steeper decreased with time, as the remnant cooled. During the Sedov phase, the turnover was at optical frequencies, while later it moved into the infrared.

b) $n_0 = 0.01$ cm^{-3} *and* $n_0 = 100$ cm^{-3}

Models B through E (see table 1) were intended to indicate how the results depend on the external medium. The value $n_0 = 0.01$ cm^{-3} is perhaps characteristic of regions outside the main disk of the Galaxy and parts of the intercloud medium. The radiated energy becomes important only at lower temperatures than in model A, and preionization of a neutral external gas is not assured. Yet it has been suggested that the low-density galactic halo is completely ionized, so the present computations, which assumed complete ionization, may be relevant. When $n_0 = 100$ cm^{-3}, as in a dense cloud, a good deal of ionizing radiation is emitted and the assumption of preionization is justified.

In run B, the magnetic postshock pressure became important before the dense shell formed; the maximum compression never increased after the adiabatic phase. At 7×10^5 years, more than 50 percent of the supernova energy had gone into the magnetic field. With the lower initial field of model C, the field became important only in the cooling region, and the magnetic energy remained small; yet it did keep the density low enough that cooling to 10° K did not occur as rapidly as it would in the absence of a field. The 10^{-5} gauss field of models D and E never became energetically important and did not impede the cooling.

In model C, the process of shell formation took place over a relatively longer time scale than in model A. The gas first cooled fairly rapidly to about 10^4 ° K (at about 6×10^5 years) with little recombination, then cooled slowly until the point when it dropped to 10° K (at about 1.3×10^6 years) and recombined. This evolution can be understood on the basis of the dip in the cooling curve at about 10^4 ° K (Dalgarno and McCray 1972).

The radiated energy of these runs (fig. 8) showed that harder radiation can be expected from an explosion in a higher density medium. The reason for this is that radiative cooling can occur at higher temperatures. At low densities, cooling proceeds by expansion rather than by radiation. The integrated energy showed the same two-peaked distribution as model A at late times (fig. 6); grains may transfer energy from the higher frequency peak to the lower. It is convenient to look at some of the properties of radiative cooling with respect to the cooling time, $t_{\rm cool}$, when the maximum density of the outer parts increases sharply. The time $t_{\rm cool}$ was 6.5×10^5, 4.2×10^4, and 4.1×10^3 years for runs C, A, and D respectively. Table 2 gives the dependence of a number of quantities on $E_0 n_0{}^2$ at time $2t_{\rm cool}$. It shows that at low $E_0 n_0{}^2$ the infrared and Lα radiation is relatively more important than the ionizing radiation, that the internal energy is more important, and that cooling sets in when the expansion is relatively more advanced. After shell formation, the appearance of the bremsstrahlung emission as a function of time was quite similar to figure 7. The luminosity/Hz of model C was about a factor 10 less than that of model A,

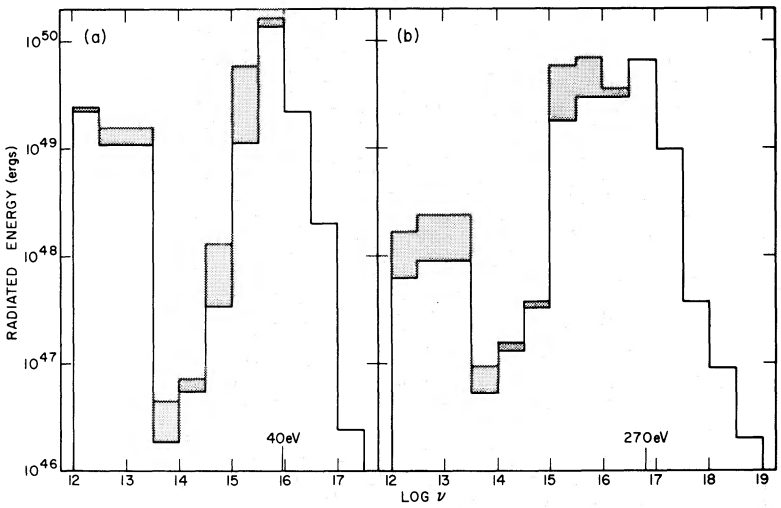

FIG. 8.—Same as fig. 6 for (*a*) model C at 2.0×10^6 years, when $1.061E_0$ has been radiated; and (*b*) model D at 1.1×10^4 years, $0.748E_0$ radiated.

TABLE 2

QUANTITIES AT $2 \times t_{cool}$

	$E_0 n_0^2$ (erg cm^{-6})		
	3×10^{46}	3×10^{50}	3×10^{54}
(L_{IR}/L_{ioniz}).....	1.8	0.38	0.0051
$(L_{L\alpha}/L_{ioniz})$.....	1.1	0.18	0.46
E_{int}/E_{kin}.....	2.3	0.54	0.43
n_c/n_0.....	3.0×10^{-4}	1.1×10^{-3}	2.3×10^{-3}
T_c (° K).....	3.6×10^{7}	8.7×10^{7}	1.4×10^{8}
v_m (km s^{-1})....	32	70	115

while that of model D was a factor 10 more. The ratio of the infrared luminosity in emission lines to that in the free-free continuum over the same wavelength region was about 1000 for model A and 30 for model D—a result of cooling at high density when the temperature is high.

In run C, the phenomenon of cooling behind the dense shell causing a pressure drop and subsequent acceleration did not occur, since the cooling times were longer than the hydrodynamic times behind the shell. The possible turbulence mentioned above seems unlikely to occur. In model E, cooling behind the dense shell was very strong and the pressure dropped more than three orders of magnitude from its central value. Acceleration by the pressure gradient might result in supersonic turbulence. An observational consequence would be bright filaments with a variety of orientations behind the dense shell.

The effect of ionizing radiation on the recombining shell was estimated in the same way as described above, and again was found not to impede shell formation. In run C, the temperature was ultimately lowered in the collapsing shell after an initial rise, and the ionized fraction was raised by a few percent. When $R = 150$ pc, the mostly neutral shell was optically thick to ionizing radiation up to an energy of 40 eV, which is rather insensitive to the radius of the shell. In run D when $R = 3$ pc, the neutral shell was optically thick to ionizing radiation below 270 eV.

Examination of the energetics of the low-density case revealed that the radiation from the hot remnant quickly became incapable of preionizing the interstellar gas. Yet the gas is likely to have an ionized fraction between 0.1 and 0.5 which characterizes the intercloud medium (Silk 1973); thus hot postshock electrons will be available to ionize neutrals. In the postshock region, although the internal energy is the same as in the preionized case, thermal energy will go into ionization energy, so the temperature and thermal pressure will be lower, resulting in a lower shock velocity. When the postshock temperature drops below about 2×10^4 ° K the cooling time for collisionally excited Lyman radiation becomes shorter than the ionization time (Kafatos 1972). The temperature will drop before ionization can take place, and the gas will move into the dense shell without having been ionized. This will occur when the shock velocity has dropped to around 35 km s^{-1}.

Expressing the radius in the form $R \sim t^q$, for run C,

$$R = 141 t_6^{0.32 \pm 0.01} \text{ pc} \qquad (t_6 > 0.75); \qquad (24)$$

and for run D

$$R = 3.46 t_4^{0.305 \pm 0.01} \text{ pc} \qquad (t_4 > 0.6), \qquad (25)$$

where t_6 and t_4 are the ages in 10^6 and 10^4 years, respectively. Extrapolation of shell velocities and kinetic energy indicated that run B would yield more than 8 percent E_0 in kinetic energy when the shell velocity reached 14 km s^{-1}, while run D would yield less than 3 percent. The difference is presumably due to the fact that at the low densities the interior loses energy not by radiation but by driving the dense shell.

Equations (20), (24), and (25) can be combined into one equation with a dependence on n_0, and the E_0 dependence can be found from the scaling law. The age can be expressed in terms of the shock velocity and radius taking $q = 0.31$, yielding

$$E_0 = 5.3 \times 10^{-7} n_0^{1.12} v_{sh}^{1.40} R^{3.12}, \qquad (26)$$

where E_0 is the initial total energy in 10^{50} ergs, n_0 is in cm^{-3}, v_{sh} in km s^{-1}, and R in pc.

As noted in § II*c*, the effects of cooling by collisionally heated grains were investigated (run E). The luminosity due to the grains was very high in the early evolution of the remnant, approaching 10^{39} ergs s^{-1}, when the temperatures were high. At a time shortly after shell formation, about 20 percent of the remnant energy had been radiated by this process. Later, the inner densities and temperatures had dropped to the point where this grain cooling was no longer significant. Because of the early loss of energy, shell formation occurred several hundred years earlier than in run D.

IV. THE EFFECT OF DENSITY INHOMOGENEITIES

It is well known that the interstellar medium is very clumpy, which undoubtedly has important consequences on the evolution of a supernova remnant. An integration, run F, was performed with a density jump from 0.1 to 5.0 cm^{-3} at a radius of 25 pc and uniform density on either side of the jump. Although the situation of a dense cloud with a spherical hole in it is physically implausible, the model may have some relevance to a situation where the cloud extends a large solid angle as seen from the point of explosion. The temperature of the low-density medium was taken to be 10^4 ° K, while that of the high-density region was chosen to keep pressure equilibrium; the interstellar gas was assumed to be preionized in the low density medium, and $x = 0.1$ in the "cloud."

Up to the point of interaction with the "cloud," the remnant was described by the adiabatic Sedov solution; but as soon as the shock entered the dense material, the shock velocity dropped from 300 to 65 km s^{-1} and cooling of the heated cloud material began (fig. 9). Simultaneously, a reflected shock moved back into the rarefied internal region. Since the shock

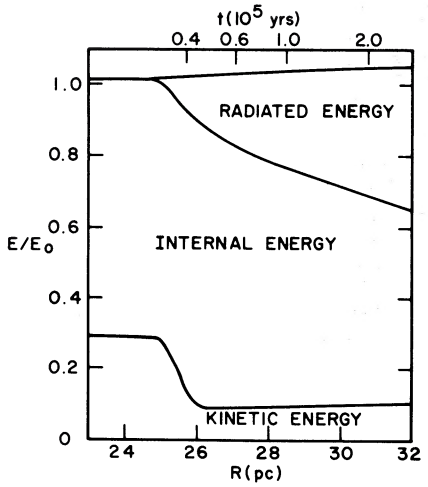

FIG. 9.—The energetics of model F as a function of radius. The density jump is at $R = 25$ pc.

velocity is proportional to $(p_2/\rho_1)^{1/2}$, where p_2 is the postshock pressure and ρ_1 is the preshock density, the shock accelerates in toward the center where the density decreases sharply. The interface between the low- and high-density material remained very sharp throughout the integration. The rise in the internal energy when the shock entered the "cloud" (fig. 9) can be attributed to the fact that while the expansion velocities were reversed in places and the kinetic energy dropped, the reflected shock heated material which had already been shocked and thus became especially hot. At later times the reflected shock reached the center of the explosion and was re-reflected; this disturbance continued to perturb the low-density region throughout the integration. The result will probably actually be turbulent motions in the low-density region.

In a more realistic situation, the shock would be expected to go around the cloud in the low-density gas (Sgro 1972). With the complication of reflections from the cloud, this flow is likely to be turbulent. As was seen in the previous section, any magnetic field present will presumably not affect the overall gas motions and will remain frozen into the gas. Thus at the edge of a cloud, a predominantly radial field might be expected.

If clouds are not dispersed by the supernova shock but cool and exist in the hot interior of the remnant, they may be energy sinks for the hot gas. Such clouds may be identified optically with low-velocity filaments in a supernova remnant. An upper limit on the luminosity due to this process can be found by assuming that the hot gas accretes at the sound velocity onto cool solar-mass clouds which are in pressure equilibrium with the hot material and which have a total mass equal to that in the dense shell. The luminosity is in the lower range of the luminosities in figure 5, using the parameters of model A. The process is probably not important energetically.

The interface between the high- and low-density material prior to being shocked is not likely to have the same shape as the incoming shock. The result will be that the shock in the dense medium is perturbed, the regions which hit the cloud first lagging behind the rest of the shock. Thus the shock will, in some places, move obliquely into the cloud. The flow of matter into an oblique shock is such as to approach the shock front (Landau and Lifshitz 1959). Non-uniformities in density and pressure can be expected across the shock front.

V. THE EFFECT OF RELATIVISTIC PARTICLES

Supernova remnants are normally identified by their nonthermal radiation, which is strong evidence for relativistic particles and magnetic fields. If the amount of material picked up by the supernova shock is large compared to the ejecta mass, it is likely that the magnetic field is intrinsic to the interstellar medium, since the time scales for magnetic diffusion are long. It is likely that this field is amplified, either by compression or by a turbulent velocity field. Three possible sources of relativistic particles are (*a*) the ambient interstellar medium; (*b*) acceleration processes associated with plasma turbulence, in particular, in shock waves; and (*c*) the initial supernova event or from a condensed object left from the explosion. It is expected that different processes will be important at different phases in the remnant evolution.

Case (*a*) has been discussed by van der Laan (1962). The continuum radiation should come from the densest, i.e., neutral, regions of the remnant. Besides the continuum radiation, ambient relativistic particles may play a role in moderating the shock wave once it has slowed down (Wentzel 1971*b*), an effect similar to that of the magnetic pressure. The quantity $p_\perp{}^2/B$, where $p_\perp$ is the relativistic particle pressure perpendicular to the magnetic field, is an adiabatic invariant. Since the cosmic-ray and magnetic pressures are comparable in the interstellar medium, the magnetic pressure should become important first behind the supernova shock.

Case (*b*) is not yet well understood, the main evidence for its occurrence being observations of the Earth's bow shock and solar radio bursts thought to be associated with MHD shocks. The main support for this process occurring in supernova shocks would be observations of strong radio emission at the outer edge of the remnant shell where the shock is expected. Also, as mentioned in § III*b*, strong cooling behind the dense shell may lead to shocks if the density is high. Gull (1973) has referred to the work of Kadomtsev and Tsytovich (1970) for the generation of cosmic rays in a turbulent region of his supernova remnant model. Yet the time scale for acceleration by this process at densities of 1 to 10 cm^{-3} appear to be prohibitively long. Also, the general expansion of the remnant should give rise to deceleration effects larger than the acceleration.

Case (*c*) has frequently been cited as giving rise to the radio radiation from very young remnants. Ostriker and Gunn (1971) have proposed that it is relativistic particles accelerated by electromagnetic fields emitted by the remnant pulsar which accelerate the supernova shell, quoting as evidence the observed acceleration of

the Crab Nebula filaments. This possibility is investigated here as an alternative to the model of Rosenberg and Scheuer (1973) in which the supernova energy is released in a spherical piston of given energy and momentum.

The innermost zone was modified to act as if filled by an adiabatic relativistic gas. Its total energy was proportional to the reciprocal of its radius, R_p, while the pressure in the zone was set equal to $E_{p0}R_{p0}/(4\pi R_p^4)$, where E_{p0} and R_{p0} are the initial total energy of relativistic particles and the radius of this zone. An infinitely thin shell of mass M_0 was included at R_p to provide for the original supernova ejecta. Integrations were performed with different initial conditions: the energy was divided between the relativistic particle energy and the kinetic energy of the thin shell, except for a small amount of energy in the next few zones out, to decrease the initial pressure difference. If the relativistic particle pressure overwhelmed the interstellar pressure in the absence of a massive shell, the interior energy would not drop as R_p^{-1}.

Figure 10 shows the energetics of three integrations with the parameters described in table 3. R_{p0} was chosen such that the effects of the interstellar medium were just becoming significant. Model G had all its initial energy in relativistic particles while that of model H was in the motion of the thin shell. For G, the energy of the relativistic particles first went into the kinetic energy of the massive shell and then into the interstellar medium. Initially the internal energy of the interstellar medium was about equal to its kinetic energy; this can be understood in that the situation approximates a highly supersonic plane piston moving into a monatomic gas, where the two energies are exactly equal. Later, the distribution of the interstellar energy tended toward that of the Sedov solution. By 1500 years, the energy of the massive shell had become negligible in both cases, and the relativistic particles began to do work directly on the interstellar gas.

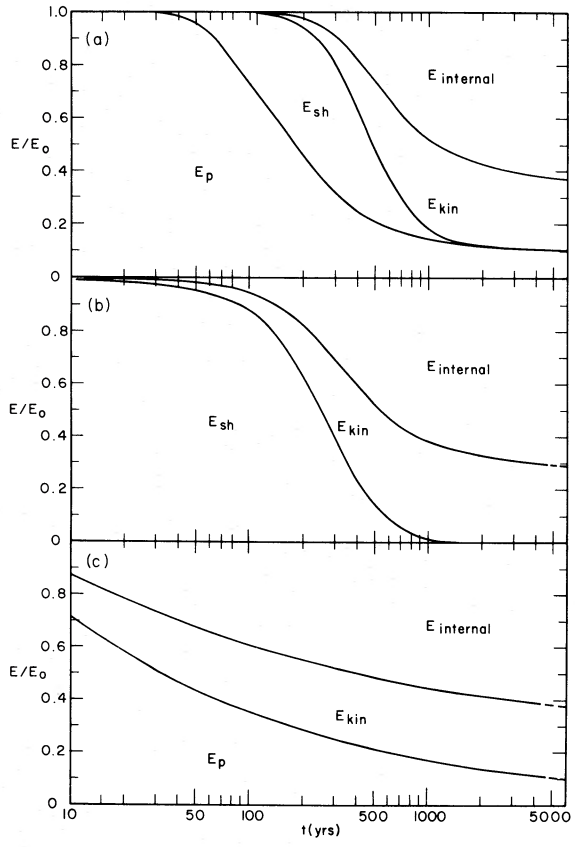

FIG. 10.—The distribution of relativistic particle energy E_p, energy in the massive shell E_{sh}, and the interstellar kinetic and thermal energy as a function of time for (*a*) model G, (*b*) model H; and (*c*) model I.

TABLE 3

MODELS OF EARLY EVOLUTION

VARIABLE	MODEL G	MODEL H	MODEL I
E_{p0} (ergs).....	1×10^{51}	0	1×10^{51}
E_{sh0} (ergs).....	0	1×10^{51}	0
M_0 ($M_\odot$).....	2.5	2.5	0
R_{p0} (pc).....	0.5	0.5	0.5
n_0 (cm^{-3}).....	1	1	1
t_{max} (years).....	6×10^3	5×10^3	5×10^3

The above analysis assumes that the cosmic-ray momentum can be transferred to the massive shell. A magnetic field frozen into the shell would have to be invoked to do this, but it may be Rayleigh-Taylor unstable, in which case the relativistic particles can leak into the interstellar medium. It is believed that cosmic rays will emit hydromagnetic waves in the interstellar medium and their momentum will be transferred to the gas (Wentzel 1971*a*; Kulsrud and Pearce 1969); the particles would be constrained to move at the Alfvén velocity, which is small compared with the shock velocity for the models considered. An integration, *I*, was performed under the assumption that they are contained, with the same initial conditions as run G except for the massive thin shell. The radius of the piston and the shock as a function of time for this model is compared with the other two models in figure 11. In I, the cavity rapidly expanded to pressure equilibrium with the interstellar medium and the pressure distribution became very much like that of the Sedov solution. Thus the shock radius increased as $t^{0.4}$, while the radius of the inner zone increased as $t^{0.3}$. By 3000 years, the shock radii were very similar in all three cases; most of the energy had been transferred to the interstellar medium. The massive shell of G had enough momentum to carry it past the cavity radius of I, but it eventually slowed and approached the radius of I. The massive shell of H eventually began to collapse; the infall is likely to be chaotic. The situation in an actual supernova remnant may be somewhere between models G and I, with a massive shell but relativistic particles outside of it.

The observational radio properties of a remnant are not predicted, due to uncertainties in the magnetic field

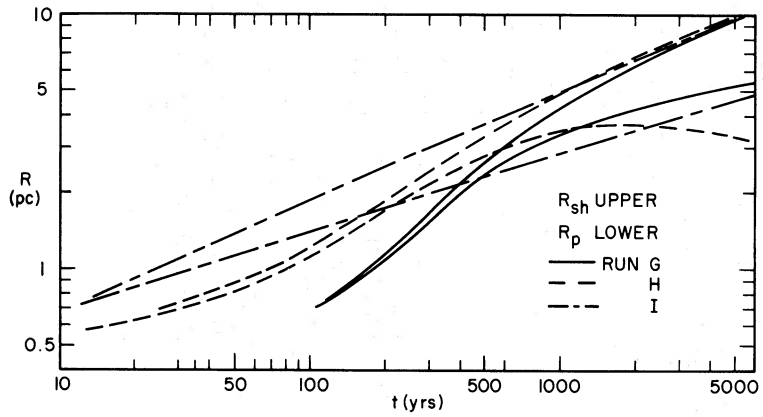

FIG. 11.—The radius of the shock, R_{sh}, and the piston, R_p, as a function of time for models G, H, and I

configuration. Very early, there may be a magnetic field associated with a condensed remnant object and the emission would be centrally located. As the expansion proceeds, this magnetic field becomes unimportant and the interstellar field may dominate, especially if there are instabilities at the interface between the supernova ejecta and the interstellar gas. Figures 10*a* and 10*c* indicate that a significant amount of energy remains in relativistic particles at later times and there will be enough in the outer regions to create a shell source. Besides the radio emission, thermal X-ray radiation is expected from the interstellar gas surrounding the relativistic particles.

Since X-rays from the shocked interstellar gas may not be easily observable whereas the interior supernova ejecta can be seen optically, it is possible to underestimate the total energy of a remnant. For example, in model G at an age of 1000 years (fig. 10*a*), the energy in the supernova ejecta was only 5 percent of the total energy, while more than 80 percent was in the interstellar medium. If relativistic particles penetrate to the outside of the ejected mass, energy is transferred to the interstellar medium even more rapidly (fig. 10*c*).

VI. COMPARISON WITH OBSERVATIONS

Due to the approximations made in this investigation, particularly that of spherical symmetry, it is not possible to make detailed comparisons with specific supernova remnants. Instead, some of the more general properties of the observations of supernova remnants will be taken up.

The scenario of observations may be as follows. The supernova remnant is initially observable as nonthermal radiation associated with a condensed object and as filamentary structures of the supernova ejecta. The explosion energy begins as relativistic particles and is transferred to the motion of the ejecta and to the interstellar medium, which is heated and emits X-rays. Instabilities at the interface between the ejecta and the interstellar medium (Gull 1973; Kulsrud *et al.* 1965) result in a region with high magnetic field which gives a shell source of nonthermal radiation as relativistic particles diffuse into the interstellar matter. As the outer parts of the remnant radiate energy, a dense neutral shell forms onto which interstellar gas accretes and cools. Compressed interstellar magnetic fields and relativistic particles will give rise to nonthermal radiation from the dense region. The original relativistic particles become less important as the remnant expands, although after much of the thermal energy has been radiated, they may again become important energetically. Hot gas inside the dense shell should be a source of X-rays.

A relation between the surface brightness and the diameter of a supernova remnant has frequently been noted (cf. Woltjer 1972) and is usually called the Σ-D relation. On the basis of the models presented here, it seems natural to interpret the nonthermal radio emission of old supernova remnants as being from compressed interstellar fields and particles in the dense cool shell, as in the model of van der Laan (1962). One objection is that the observed radio shells are quite thick (Willis 1972) and there is insufficient compression to give the observed radio intensity. Yet this may be due to poor resolution; for the Cygnus Loop, which has been observed at high resolution (Moffat 1971), the above model may account for the radio radiation. As for the large thickness of many radio shells, it may be that there are filamentary structures at a range of radii from the center of the blast, as would be expected for a shock moving in a clumpy medium (Sgro 1972).

If η (defined in eq. [15]) is greater than 10, the interstellar emissivity will be increased by a factor of about (Moffat 1971)

$$(\tfrac{1}{2}\eta \sin\phi)^{1-\alpha}\{\tfrac{1}{3}\eta[0.5 + 0.65(\eta/2)^{1/2}]^{-2\alpha}\}, \quad (27)$$

where ϕ is the angle between the B field and the expansion velocity and α is the spectral index; the expression is essentially from van der Laan (1962). The first term is from the compression of the magnetic field, and the second is from the compression of the relativistic particles. Thus, for sufficiently large η,

$$\Sigma \sim R\eta^{1-2\alpha}. \quad (28)$$

Equation (17) shows that η is proportional to v_{sh} in

the standard model, provided the Alfvén velocity in the interstellar medium remains constant. Thus if $R \sim t^q$,

$$\Sigma \sim R^{(1-1/q)(1-2\alpha)+1} . \quad (29)$$

A typical value for α might be -0.5, while q must lie between 0.4 (Sedov solution) and 0.25 (momentum conservation). If $\Sigma \sim D^n$, n lies between 2 and 5, with $n = 3.44$ for $q = 0.31$ as found from a fit to computations in § III*a*. In the inhomogeneous interstellar medium it is difficult to accurately estimate q; but if dense condensations are forming, one would expect n to be close to the upper limit. Values of n deduced from observation include 3.7, 2.7, 4.5, and 3.6 (Woltjer 1972 and references therein); 4.0 ± 0.2 (Ilovaisky and Lequeux 1972); and 3.0 (Mathewson and Clarke 1973). Differences in the initial explosion energy and the nature of the surrounding interstellar density and magnetic field will cause deviations from the law. Taking $q = 0.31$, $\alpha = -0.5$, and the dependences of E_0 and n_0 of the physical quantities at the transition time to the dense shell from Cox (1972*b*), Σ is proportional to $E_0^{1.4} n_0^{-0.60} B_0^{-2.0}$, and to the emissivity of the surrounding gas.

Observational estimates of the pressure in a supernova remnant can be made if densities and temperatures are derived from the emission-line intensities of one ion. Miller (1974) has recently made detailed spectroscopic measures of filaments in the Cygnus Loop and in one filament was able to derive $T_e = 8400°$ K and $n_e = 1180\ \mathrm{cm}^{-3}$ from the [S II] lines alone, implying a lower limit to the pressure of 2.74×10^{-9} g cm^{-1} s^{-2} in the region giving rise to these lines. Assuming a radius of 20 pc for the Cygnus Loop (which may be an underestimate considering the radio emission in the southwest part of the nebula), the energy in the blast is

$$E_0 = 1.46 \times 10^{60} (\beta p_{\mathrm{obs}}/\xi)\ \mathrm{ergs} , \quad (30)$$

where β is the ratio of the mean pressure in the remnant to the observed pressure, p_{obs}, and ξ is the ratio of the total thermal energy to the total initial energy of the blast. In the early stages of the models presented here, β is never less than about $\frac{1}{3}$, although later the dense shell becomes more dissociated from the hot interior and β can be smaller. Considering the high velocities of the Cygnus Loop filaments (100 km s^{-1}), it seems unlikely that β is below $\frac{1}{3}$. The quantity ξ varies from 0.7 on down. Taking $\xi = 0.35$ and $\beta = 0.33$ with the above p_{obs}, we find

$$E_0 \approx 4 \times 10^{51}\ \mathrm{ergs} , \quad (31)$$

which is considerably greater than the 4×10^{50} ergs suggested by Cox (1972*c*). It is possible that the value of β was overestimated due to the imposition of spherical symmetry; perturbations of the shock front due to density inhomogeneities may well cause pressure gradients across the front. X-ray observations definitely favor the lower energy (Cox 1972*c*). If $E \approx 10^{51}$ ergs is typical of supernova explosions, they may provide all the kinetic energy to the interstellar medium (Woltjer 1972).

The results in § III indicate that supernova remnants should emit infrared radiation due to (*a*) line emission from the low-temperature gas, (*b*) continuum emission from radiation-heated grains, (*c*) continuum emission from collisionally heated grains, and (*d*) free-free emission. Large amounts of energy may be radiated by the first three mechanisms. The only definite supernova remnant which has been observed in the infrared is W28 (Hoffman, Fredrick, and Emery 1971); Milne and Wilson (1971) describe the remnant. Considering that the observed source is a knot at the edge of the supernova remnant and that the wavelength band used by Hoffman *et al.* is centered on 100 μ, the emission is probably by mechanism (*b*). Further attempts at supernova remnant observations in the infrared would seem warranted, especially since remnants can be detected over great distances at these wavelengths. It is possible that infrared sources observed near the galactic center are associated with the remnant of a strong explosion (Scoville 1972).

As has been noted before (e.g., Cox 1972*b*), most of the remnant mass of the models is in neutral hydrogen. It is distributed in a thin shell whose thickness depends on the shock velocity and the interstellar conditions, especially the magnetic field. A shell of H I has been observed around HB 21 (Assousa and Erkes 1973). A line of sight through the edge of model A at 1×10^5 years would be optically thick in the 21-cm line, and the observed brightness temperature would be the actual temperature of the gas, which is 10° K in the present models, but is probably not reliable. The ratio of the column density at the edge of the shell to that at the center is proportional to η. The column density at the center, which will have the largest velocity relative to the local gas, is approximately the radius of the remnant times the interstellar density. The velocity dispersion in the model shells is several km s^{-1}; in an inhomogeneous medium, larger dispersions can be expected.

VII. CONCLUSIONS

The following conclusions are indicated by the present investigation:

1. Models intended to cover the parameters of initial explosion energy and ambient density can be reduced to a one-parameter set of models using a scaling law.
2. In the late stages of a supernova remnant, a dense neutral shell forms at the outer edge which is optically thick to hard-ultraviolet radiation. The frequency at which the shell becomes thin increases with the density of the ambient gas.
3. In the absence of heating mechanisms besides the ionizing radiation, the shell will cool to 10° K; thus a significant amount of the supernova energy will be radiated in infrared lines.
4. As long as the pressure of the postshock magnetic field is less than the ram pressure, a magnetic field does not affect the dynamics but only the maximum density in the dense shell and its thickness.

5. An explosion in a high-density medium will emit a larger proportion of hard radiation than one in a low-density medium.

6. An explosion in a low-density medium is especially efficient at converting the explosion energy to kinetic energy of clouds. The efficiency can be 8 percent when the dense shell has slowed to 14 km s^{-1} (model C).

7. Material accretes onto both sides of the dense shell. A turbulent region associated with cooling behind the dense shell may occur, especially at high densities.

8. If the explosion takes place in a cloud, a significant amount of the energy (about 20 percent for run E) can be radiated in the infrared in the early stages due to radiation from grains heated by collisions with the gas.

9. In hitting a large cloud, much of the kinetic energy of the remnant is lost, as opposed to the thermal energy which increases due to the reflected shock. The interface between the high- and low-density material remains distinct after the penetration.

10. Assuming the supernova energy is deposited as relativistic particles, the ratio of the radius of the heated interstellar gas to the radius of the region with relativistic particles rises as $t^{0.1}$ once the two regions have reached pressure equilibrium. The total energy of a supernova remnant in its early stages may be underestimated if the energy in the heated interstellar gas is not taken into account.

11. The Σ-D relation can be explained using van der Laan's theory for the radio emission as arising from compressed interstellar magnetic fields and relativistic gas. It is conjectured that currently most supernova remnants are far from being resolved at radio frequencies; the shells appear thick due to many thin filaments at varying distances from the center of the remnant.

I am deeply indebted to my thesis advisor, J. P. Ostriker, for many stimulating discussions. Joe Schwarz provided valuable guidance on the one-dimensional hydrodynamic code and the physics of the interstellar medium. Robert Stein kindly made available the basic code. Conversations with K. Davidson, E. Jenkins, R. Kulsrud, P. Mészáros, F. Perkins, and L. Spitzer were very helpful, as was correspondence with D. Cox and W. C. Straka. I was supported by a National Science Foundation Graduate Fellowship during the course of this work.

REFERENCES

Assousa, G. E., and Erkes, J. W. 1973, *Bull. AAS.*, **5**, 322.
Auer, L. H. 1966, thesis, Princeton University.
Bethe, H. A., and Salpeter, E. E. 1957, *Quantum Mechanics of One- and Two-Electron Atoms* (New York: Academic Press).
Brown, R. L. 1971, *Ap. J.*, **164**, 387.
Burke, J. R., and Silk, J. 1974, in preparation.
Cox, D. P. 1972*a*, *Ap. J.*, **178**, 143.
———. 1972*b*, *ibid.*, p. 159.
———. 1972*c*, *ibid.*, p. 169.
Cox, D. P., and Daltabuit, E. 1971, *Ap. J.*, **167**, 113.
Cox, D. P., and Tucker, W. H. 1969, *Ap. J.*, **157**, 1157.
Dalgarno, A., and McCray, R. 1972, *Ann. Rev. Astr. and Ap.*, **10**, 375.
Field, G. B., Rather, J. D. G., Aannestad, P. A., and Orzag, S. A. 1968, *Ap. J.*, **151**, 953.
Gull, S. F. 1973, *M.N.R.A.S.*, **161**, 47.
Hoffman, W. F., Frederick, C. L., and Emery, R. J. 1971, *Ap. J.* (*Letters*), **170**, L89.
Ilovaisky, S. A., and Lequeux, J. 1972, *Astr. and Ap.*, **18**, 169.
Jura, M., and Dalgarno, A. 1972, *Ap. J.*, **174**, 365.
Kadomtsev, B. B., and Tsytovich, V. N. 1970, *IAU Symposium 39* (Dordrecht: Reidel), p. 108.
Kafatos, M. C. 1972, thesis, Massachusetts Institute of Technology.
Kulsrud, R. M., Bernstein, I. B., Kruskal, M., Fanucci, J., and Ness, N. 1965, *Ap. J.*, **142**, 491.
Kulsrud, R. M., and Pearce, W. P. 1969, *Ap. J.*, **156**, 445.
Landau, L. D., and Lifshitz, E. M. 1959, *Fluid Mechanics* (London: Pergamon).
Mathewson, D. S., and Clarke, J. N. 1973, *Ap. J.*, **180**, 725.
Michel, F. C., and Yahil, A. 1973, *Ap. J.*, **179**, 771.
Miller, J. 1974, in preparation.
Milne, D. K., and Wilson, T. L. 1971, *Astr. and Ap.*, **10**, 220.
Moffat, P. H. 1971, *M.N.R.A.S.*, **153**, 401.
Oster, L. 1961, *Ap. J.*, **134**, 1010.
Ostriker, J. P., and Gunn, J. E. 1971, *Ap. J.* (*Letters*), **164**, L95.
Ostriker, J. P., and Silk, J. 1973, *Ap. J.* (*Letters*), **184**, L113.
Rosenberg, I., and Scheuer, P. A. G. 1973, *M.N.R.A.S.*, **161**, 27.
Schwarz, J. 1973, *Ap. J.*, **182**, 449.
Schwarz, J., McCray, R., and Stein, R. F. 1972, *Ap. J.*, **175**, 673.
Scoville, N. Z. 1972, *Ap. J.* (*Letters*), **175**, L127.
Sedov, L. I. 1959, *Similarity and Dimensional Methods in Mechanics* (New York: Academic Press).
Sgro, A. 1972, thesis, Columbia University.
Shapiro, S. L. 1973, *Ap. J.*, **185**, 69.
Silk, J. 1973, *Ap. J.*, **181**, 707.
Spitzer, L. 1948, *Ap. J.*, **107**, 6.
———. 1962, *Physics of Fully Ionized Gases* (New York: Interscience).
———. 1968, *Diffuse Matter in Space* (New York: Interscience).
Straka, W. C., Goldreich, P., and Sargent, W. 1971, *Bull. AAS*, **3**, 451.
Taylor, G. I. 1950, *Proc. R. Soc. London*, **A201**, 159 and 175.
Tucker, W. H., and Koren, M. 1971, *Ap. J.*, **168**, 283.
van der Laan, H. 1962, *M.N.R.A.S.*, **124**, 125.
Wentzel, D. G. 1971*a*, *Ap. J.*, **163**, 503.
———. 1971*b*, *ibid.*, **170**, 53.
Wiese, W. L., Smith, M. W., and Glennon, B. M. 1966, *Atomic Transition Probabilities*, Vol. **1** (NSRDS).
Willis, A. G. 1972, thesis, University of Illinois.
Woltjer, L. 1972, *Ann. Rev. Astr. and Ap.*, **10**, 129.

Note added in proof.—It should be pointed out that the radius referred to in equations (20), (24), and (25) is the shock radius and not a mass-weighted radius for the dense shell. This is the reason for q being different from 0.25 as expected by momentum conservation, which is approximately valid at late times (after 1.4×10^5 years for model A). I am indebted to W. C. Straka for commenting on this.